LETTERS
PUBLISHED ONLINE: 18 MAY 2015 | DOI: 10.1038/NPHOTON.2015.79
nature photonics

Limitations of nonlinear optical isolators due to dynamic reciprocity

Yu Shi[1], Zongfu Yu[2] and Shanhui Fan[1]*

Motivated by the demands of integrated and silicon photonics, there is significant interest in optical isolators in on-chip integrated systems. Recent works have therefore explored nonlinear optical isolators and demonstrated non-reciprocal transmission contrast when waves are injected in forward or backward directions[1–8]. However, whether such nonlinear isolators can provide complete isolation under practical operating conditions remains an open question. Here, we analytically prove and numerically demonstrate a dynamic reciprocity in nonlinear optical isolators based on Kerr or Kerr-like nonlinearity. We show that, when a signal is transmitting through, such isolators are constrained by a reciprocity relation for a class of small-amplitude additional waves and, as a result, cannot provide isolation for arbitrary backward-propagating noise. This result points to an important limitation on the use of nonlinear optical isolators for signal processing and for laser protection.

To build an optical isolator one needs a mechanism to break Lorentz reciprocity[9,10]. The standard approach is to use magneto-optical materials that possess an asymmetric permittivity tensor[11–17]. In an alternative approach (that is attractive for on-chip integration in particular), it has been shown that one can completely reproduce the effect of magneto-optics using non-magnetic structures undergoing spatiotemporal modulation[18–27]. Both approaches result in linear isolators with responses that are independent of the amplitude of the input signal.

In contrast to linear isolators, one can instead break the Lorentz reciprocity using nonlinearity (for example, Kerr or Kerr-like nonlinearity[9,10]). Many recent works have reported the construction of nonlinear optical isolators[1–8]. To demonstrate non-reciprocity in these isolators, an input wave is typically launched within a particular power range—either forward or backward—to demonstrate high transmission in the forward and low transmission in the backward directions. However, an ideal isolator needs to suppress the transmission of arbitrary waves in the backward direction, independent of whether there is an input wave in the forward direction or not. For nonlinear isolators it has been hypothesized that in the situation where a strong forward input is being transmitted, there may be significant transmission for weak backward waves[8,15]. Throughout this Letter we will refer to such forward input as the 'signal' and the weak additional input wave that is injected when the strong forward input is present as the 'noise'. The existence of such backward noise transmission would significantly limit the suitability of nonlinear optical isolators for many applications, for example where an isolator is used to protect a laser source from reflected noises, or in the context of optical communication where the backward noise may arrive when a forward signal is passing through the isolator. However, there been no theoretical proof of such a hypothesis, nor has there been any numerical or experimental work on such a scenario. As a result, it is unclear whether such a limitation is generally present for nonlinear optical isolators.

In this Letter, we present a formal proof of a dynamic reciprocity in nonlinear optical isolators where the Lorentz reciprocity is broken by Kerr nonlinearities. For such devices, we demonstrate that in the presence of a strong forward signal there is a class of band-limited noises for which the device is in fact reciprocal. Thus, in the presence of a strong forward signal, the isolator cannot suppress the transmission of arbitrary noise in the backward direction. The proof is completely general and independent of the device geometry. We validate the proof by a direct first-principles simulation of a nonlinear optical isolator.

We start with a brief review of the operating principle of nonlinear optical isolators. Such devices, by necessity, have a spatially asymmetric linear permittivity profile $\varepsilon(\mathbf{r})$ (Fig. 1a). Without nonlinearity, the system is reciprocal[9,10]. The input waves travelling forward and backward have the same transmission coefficients, and the linear permittivity profile is typically chosen such that the transmission is low. However, because $\varepsilon(\mathbf{r})$ is spatially

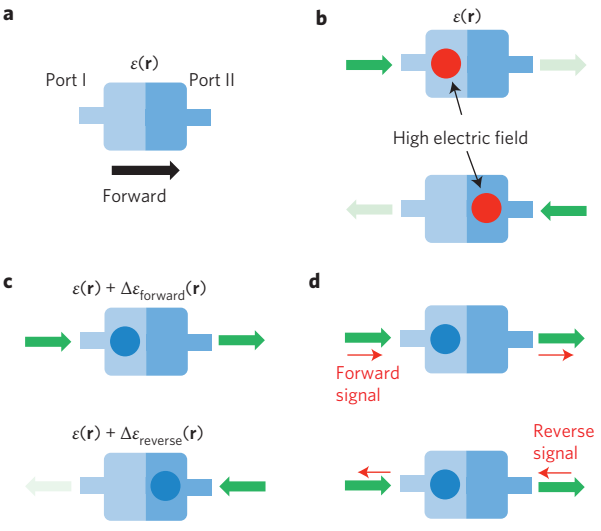

Figure 1 | Operating principle for a nonlinear optical isolator. a, A two-port device with a linear permittivity profile $\varepsilon(\mathbf{r})$ that is spatially asymmetric. **b**, Without nonlinearity, an input beam entering from either port has the same transmission coefficients, but may excite different field distributions within the device. **c**, With nonlinearity, the forward and backward waves see different dielectric permittivity distributions. In the forward direction, the permittivity distribution is favourable for transmission, whereas in the reverse direction, the permittivity distribution is not favourable for transmission, resulting in a nonlinear optical isolator. **d**, Schematics of reciprocity analysis for small additional waves in the presence of a large forward signal. The structure is reciprocal for the small additional waves in the presence of a large forward signal.

[1]Department of Electrical Engineering, Ginzton Laboratory, Stanford University, Stanford, California 94305, USA. [2]Department of Electrical and Computer Engineering, University of Wisconsin, Madison, Wisconsin 53706, USA. *e-mail: shanhui@stanford.edu

asymmetric, fields may concentrate in different locations for forward and backward waves (Fig. 1b). When nonlinearity is introduced, because the dielectric properties now depend on the field strength, the forward and backward waves see different dielectric structures, and thus the system becomes non-reciprocal (Fig. 1c). As a result, one can design the system to exhibit high transmission for an input forward signal with sufficiently high power, while maintaining low transmission for backward waves. Such nonlinear non-reciprocity has been observed in many experiments[1–3].

In most experiments on nonlinear isolators one has either forward or backward waves, but not both. In contrast, as argued above, we consider transmission of the backward noise in the presence of a high-power forward signal (Fig. 1d). For this purpose, we consider the transmission of a small additional wave input in the presence of a high-power forward signal, in both the forward and backward directions. Because the forward signal has a high transmission coefficient, by continuity the small additional wave input along the forward direction should also have high transmission. On the other hand, the behaviour of the small additional wave input can, in general, be obtained by linearizing the nonlinear Maxwell's equation around the solution that corresponds to the high-power forward signal. If the resulting linearized equation is reciprocal, its transmission property must be symmetric and hence the backward noise would also have high transmission. Therefore, the transmission of the backward noise can be inferred by considering the reciprocity of the linearized equation.

We have developed a linearized equation that governs the propagation of a small-amplitude additional wave in the presence of a large-amplitude signal. The electric field $\tilde{\mathbf{E}}$ is described by the following equation in the time domain[28]:

$$\nabla\times\nabla\times\tilde{\mathbf{E}}+\mu_0\epsilon(\mathbf{r})\frac{\partial^2\tilde{\mathbf{E}}}{\partial t^2}=-\mu_0\frac{\partial^2\tilde{\mathbf{P}}^{\mathrm{NL}}}{\partial t^2} \quad (1)$$

where $\tilde{\mathbf{P}}^{\mathrm{NL}}$ represents the nonlinear polarization density, as can be derived from Maxwell's equations (Supplementary Section I). In this Letter, fields with and without a '~' over represent a signal in time or the complex amplitude of a time-harmonic signal, respectively. Furthermore, all fields have implicit spatial $\mathbf{r}$ dependence. For our purpose, we consider the field in the system to have the following form (Fig. 2a):

$$\tilde{\mathbf{E}}=\mathbf{E}_0e^{i\omega_0t}+\mathbf{E}_se^{i\omega_st}+\mathrm{c.c.} \quad (2)$$

where the first term represents a large-amplitude signal at frequency ω_0 and the second term represents a small additional wave at frequency ω_s with $|\mathbf{E}_s|\ll|\mathbf{E}_0|$.

We consider the effect of an instantaneous Kerr nonlinearity, as has been assumed in a number of studies on nonlinear optical isolators[1–8]. The nonlinear polarization density $\tilde{\mathbf{P}}^{\mathrm{NL}}$ then has the form

$$\tilde{\mathbf{P}}^{\mathrm{NL}}=\epsilon_0\chi^{(3)}(\mathbf{r})\tilde{\mathbf{E}}^3 \quad (3)$$

For the electric field in equation (2), the polarization density becomes

$$\tilde{\mathbf{P}}^{\mathrm{NL}}=\epsilon_0\chi^{(3)}(\mathbf{r})(\mathbf{E}_0e^{i\omega_0t}+\mathbf{E}_se^{i\omega_st}+\mathrm{c.c.})^3 \quad (4)$$

Because the small signal amplitude is much less than the large forward wave amplitude, we can linearize the system by ignoring higher-order $\mathbf{E}_s$ components. When focusing the analysis on the small additional wave with frequency ω_s, equation (4) reduces to

$$\mathbf{P}^{\mathrm{NL}}(\omega_s)\cong 6\epsilon_0\chi^{(3)}(\mathbf{r})|\mathbf{E}_0|^2\mathbf{E}_s \quad (5)$$

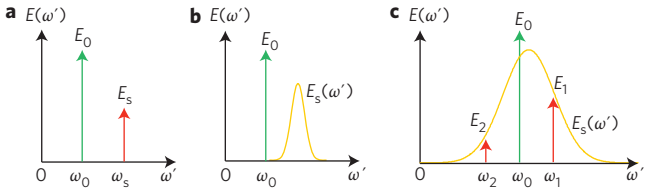

Figure 2 | Frequency spectra of various input waves for a nonlinear optical isolator. The green arrow represents the large-amplitude signal. A red arrow represents a CW. component of a small-amplitude additional wave. The yellow curve represents the small-amplitude additional wave, which has a non-zero spectral bandwidth. **a**, The small-amplitude additional wave only has a single frequency component away from the large-amplitude signal. **b**, The small-amplitude additional wave has a spectral band with a non-zero bandwidth but does not overlap with the large-amplitude signal. **c**, The small-amplitude additional wave has a spectral band that overlaps with the large-amplitude signal. With respect to the small-amplitude additional wave, the system is reciprocal in cases **a** and **b** and non-reciprocal in case **c**.

Combining equation (5) with the nonlinear wave equation in equation (1), we obtain the linearized equation for the small additional wave:

$$\nabla\times\nabla\times\mathbf{E}_s-\omega_s{}^2\mu_0\left[\epsilon(\mathbf{r})+6\epsilon_0\chi^{(3)}(\mathbf{r})|\mathbf{E}_0|^2\right]\mathbf{E}_s=0 \quad (6)$$

In the presence of the large forward signal, we see that the field of the small signal satisfies an equation that is of the same form as Maxwell's equation, with the dielectric function modified as $\epsilon(\mathbf{r})\rightarrow\epsilon(\mathbf{r})+6\epsilon_0\chi^{(3)}(\mathbf{r})|\mathbf{E}_0|^2$. Because the modified dielectric function remains scalar and time-independent, the resulting linearized equation is reciprocal[9,10]. In this Letter we refer to such a reciprocity arising in the linearized equation for a nonlinear system as a 'dynamic reciprocity'. The term 'dynamic' is used to signify the presence of a forward signal and to differentiate from the standard Lorentz reciprocity, because the nonlinear system is non-reciprocal in general. As a result of such dynamic reciprocity, in the presence of the large forward signal, which has high transmission, the small noise in the backward direction also has high transmission. Hence, the device cannot provide complete optical isolation in such a scenario.

We make a few comments on the above proof of dynamic reciprocity. First, the proof here is completely general and structure-independent. In particular, $\epsilon(\mathbf{r})$ can be complex. The proof therefore applies to systems with gain or loss and in particular to nonlinear optical isolators with parity–time symmetry, as considered in refs 2, 3, 6 and 7. Also, we have only considered optical isolators, which are two-port devices, but the same dynamic reciprocity exists for multi-port nonlinear non-reciprocal devices, such as nonlinear circulators. Furthermore, although our proof here assumes instantaneous Kerr nonlinearity, the same equation (6) also arises for thermo-optic nonlinearity. Hence, the conclusion here also holds for the experimental systems considered in refs 1 and 4. Finally, our proof assumes continuous-wave (CW) noise (Fig. 2a), but the proof can be generalized to the case where the noise occupies a spectral band with a non-zero bandwidth, but with no spectral overlap with the forward signal (Fig. 2b). Such a noise spectrum is important practically in optical systems. For example, in laser applications the reflected light may have a frequency that is slightly shifted from the laser light due to time-dependent environmental fluctuations. The feedback of such frequency-shifted reflected light into the laser then results in increased frequency noise due to the frequency-pulling effect[29]. A common use of optical isolators is to suppress such feedback. On the other hand, in the case with instantaneous Kerr nonlinearity, for a small

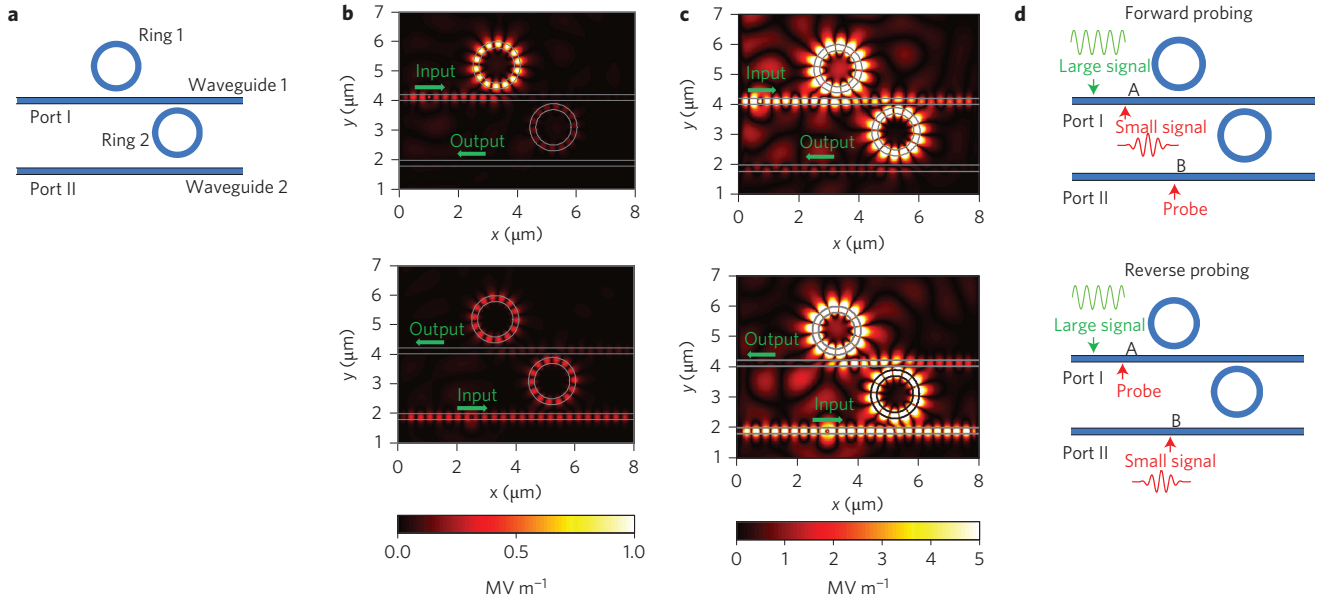

Figure 3 | Simulation of a nonlinear optical isolator. a, Schematics of the simulated structure consisting of two waveguides and two ring resonators. **b**, Electric field distributions inside the structure for forward (top) and backward (bottom) waves, in the absence of nonlinearity. The transmission in both directions is low, but we observe a discrepancy between these two field patterns within the structure. **c**, Electric field distributions inside the structure for forward (top) and backward (bottom) waves, in the presence of nonlinearity. The top panel shows visible forward transmission coming out of port II, whereas the bottom figure shows very little reverse transmission coming out of port I. **d**, Schematics of the set-up for testing reciprocity for small additional input waves in the presence of a large forward signal. For forward analysis, the small additional wave is excited at point A and probed at point B to measure the forward transmission spectrum (top). For backward analysis, signal is sent from point B and probed at point A to measure the backward transmission spectrum (bottom).

additional wave whose frequency spectrum overlaps with the frequency of the large forward signal (Fig. 2c), the resulting linearized equation is non-reciprocal (see Supplementary Section II for a detailed explanation).

To validate the above theoretical analysis, we performed two-dimensional finite-difference time-domain (FDTD) simulations on a class of nonlinear optical isolators proposed and demonstrated in ref. 1. Our structure contains two straight waveguides and two ring waveguides as shown in Fig. 3. The widths of all waveguides are 200 nm and the radii of both ring waveguides, measured at the centres of the waveguides, are 700 nm. The relative permittivity of the waveguides is 12, and they are surrounded by vacuum with a relative permittivity of 1. For ring 1, critical coupling via radiation loss is achieved at $\lambda_{crit} = 1{,}677.2$ nm by setting the gap between ring 1 and waveguide 1 to $G_{11} = 184$ nm. In ring 2, the gaps between ring 2 and waveguides 1 and 2 are set to $G_{21} = 111$ nm and $G_{22} = 314$ nm, respectively. Ring 2 is used to achieve an attenuated transfer between the two waveguides, and the transfer efficiency also peaks at $\lambda = 1{,}677.2$ nm. The forward direction is defined as going from port I to port II, and vice versa for the reverse direction. In the FDTD simulation, the resolution in the x and y directions is $h_x = h_y = 25$ nm and the resolution in time is $h_t = 0.059$ fs. Perfectly matched layers are used to surround the simulation domain[30].

In the simulations we calculate the power transmission coefficients between the input and output waveguides. Importantly, because both the input and output waveguides are single-moded, such power transmission coefficients are the same as the modal transmission coefficients discussed by Jalas and co-authors[9]. Comparing such transmission coefficients along the forward and backward directions is then a direct test of reciprocity. Our numerical set-up is equivalent to the experimental set-up proposed by Jalas and colleagues, with the single-mode waveguides in our case playing the role of a modal filter[9].

First, we show forward and backward propagation in this structure in the absence of optical nonlinearity (Fig. 3b). Because ring 1 is critically coupled at the operating wavelength, transmission is close to zero in both the forward and backward directions. Nevertheless, we notice a difference in field distribution for the two propagation directions. For forward propagation, the fields are much more highly concentrated in ring 1.

For the case with nonlinearity we incorporate optical Kerr nonlinearity into both rings with $\chi^{(3)} = 2.8 \times 10^{-18}$ m^2 V^{-2} and apply a large current source at either port I or port II, such that the input guided power is 10.4 mW μm^{-1}. During the simulation, a nonlinear FDTD update algorithm is adopted for the regions with nonlinearity[31]. With the Kerr nonlinearity introduced, at the same frequency as considered above, for the forward direction, the high field concentration in ring 1 will slightly shift the resonance frequency of ring 1, such that the wave can pass through ring 1 and be transferred into port II, thus attaining non-zero transmission. For the backward direction the field concentration in ring 1 is not as strong and, as a result, the structure provides low transmission (Fig. 3c). The structure therefore behaves as a nonlinear optical isolator.

We now numerically demonstrate the dynamic reciprocity for such nonlinear isolators according to the simulation set-up in Fig. 3d. First, the same large signal is applied at port I as in Fig. 3c, which results in high transmission to port II. Once the field in the computation domain reaches the steady state, we introduce a small additional band-limited pulse in either the forward or backward directions and probe their transmission spectra, while maintaining the large forward input signal unchanged. For analysis in the forward direction, the small additional pulse is excited via a source at point A, and the transmitted field is detected at point B. In the backward analysis, the same pulse is excited at point B and detected at point A.

The amplitude of the small additional input pulse is chosen to have the form of $\mathrm{sinc}^2(t)$ in time, so that the input pulse spectrum has a band-limited triangular shape. Such an input spectrum is denoted $E_{s,ref}(\lambda)$ (Fig. 4a). The parameter of this additional input pulse is chosen such that its spectrum has no overlap with the

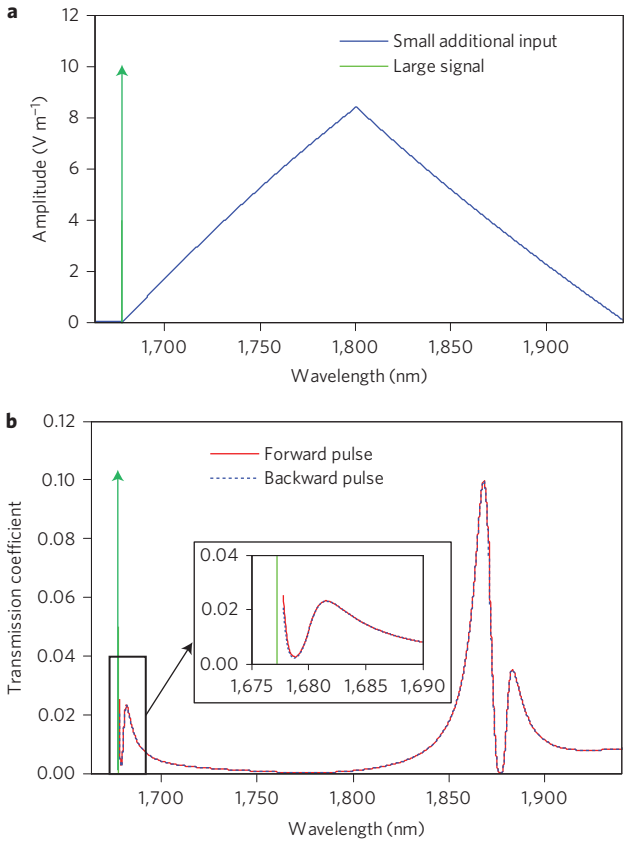

Figure 4 | Numerical demonstration of dynamic reciprocity. a, Spectrum of the small additional input pulse in Fig. 3c probing the forward and backward transmission coefficient. The pulse is designed to peak at $\lambda = 1{,}800$ nm and it is non-zero starting from $\lambda = 1{,}677.7$ nm, which is 0.5 nm away from the wavelength of the large signal. **b**, Plot of the forward and backward transmission coefficients for such a small additional input pulse. The forward and backward transmission coefficients are identical to each other.

frequency of the large CW input signal. From the transmitted field due to the additional forward and backward small pulses (labelled $E_{s,fwd}(t)$ and $E_{s,bkw}(t)$, respectively), we obtain the corresponding spectra $E_{s,fwd}(\lambda)$ and $E_{s,bkw}(\lambda)$. The forward and backward transmission coefficients for the small additional inputs can then be found as

$$T_{fwd}(\lambda) = \left|\frac{E_{s,fwd}(\lambda)}{E_{s,ref}(\lambda)}\right|^2, T_{bkw}(\lambda) = \left|\frac{E_{s,bkw}(\lambda)}{E_{s,ref}(\lambda)}\right|^2 \quad (7)$$

and are plotted in Fig. 4b. We observe $T_{fwd}(\lambda) = T_{bkw}(\lambda)$ for all λ where the small additional input pulse has non-zero amplitude. The numerical simulations indeed demonstrate that this nonlinear optical isolator has a dynamic reciprocity, as we predict by theoretical analysis.

In this Letter we have focused on nonlinear optical isolators based on Kerr or Kerr-like nonlinearity. The analysis procedure and the concept of dynamic reciprocity should also be relevant, in general, for other types of nonlinear optical isolator. For example, we have performed a similar analysis for an isolator based on the second-order nonlinear effect[32]. The result indicates that such a structure is also constrained by the same dynamic reciprocity. Hence, there is a class of backward-propagating noise that cannot be blocked by such a nonlinear isolator when there is a forward signal passing through the structure. Finally, we note that there are optical isolators based on nonlinear optical effects such as stimulated Brillouin scattering (SBS)[33,34] that are in fact linear in their response with respect to the signal field, and are therefore not subject to the limitation we discuss here.

In conclusion, we have analytically proved and numerically demonstrated dynamic reciprocity in a nonlinear optical isolator based on Kerr and Kerr-like nonlinearity. We show that when a signal is being transmitted through a nonlinear optical isolator, the isolator is in fact reciprocal for a class of small-amplitude additional waves. Thus, the nonlinear isolator cannot block a class of small-amplitude noise in the backward direction when a forward signal is being transmitted through it. In system applications, isolators are used to suppress unknown backward noise. Therefore, as emphasized by Jalas and colleagues[9], 'For a device to be an isolator it must block or divert all possible states for backward propagation.' By showing that there is a large set of backward propagation states that the nonlinear isolator cannot block, we have proved that the nonlinear isolator in fact cannot function as an isolator. Here, for concreteness, we have focused only on nonlinear optical isolators based on Kerr and Kerr-like nonlinearity, but our work points to the importance of the concept of dynamic reciprocity in general. We anticipate that the conclusion that there is a class of backward propagating states that nonlinear isolators cannot block holds true for a much broader set of nonlinear optical isolators than we consider here.

Received 19 November 2014; accepted 14 April 2015; published online 18 May 2015

References

1. Fan, L. *et al.* An all-silicon passive optical diode. *Science* **335,** 447–450 (2012).
2. Peng, B. *et al.* Parity–time-symmetric whispering-gallery microcavities. *Nature Phys.* **10,** 394–398 (2014).
3. Chang, L. *et al.* Parity–time symmetry and variable optical isolation in active–passive-coupled microresonators. *Nature Photon.* **8,** 524–529 (2014).
4. Wang, J. *et al.* A theoretical model for an optical diode built with nonlinear silicon microrings. *J. Lightw. Technol.* **31,** 313–321 (2013).
5. Miroshnichenko, A., Brasselet, E. & Kivshar, Y. Reversible optical nonreciprocity in periodic structures with liquid crystals. *Appl. Phys. Lett.* **96,** 063302 (2010).
6. Bender, N. *et al.* Observation of asymmetric transport in structures with active nonlinearities. *Phys. Rev. Lett.* **110,** 234101 (2013).
7. Nazari, F. *et al.* Optical isolation via PT-symmetric nonlinear Fano resonances. *Opt. Express* **22,** 9574–9584 (2014).
8. Fan, L. *et al.* Silicon optical diode with 40 dB nonreciprocal transmission. *Opt. Lett.* **38,** 1259–1261 (2013).
9. Jalas, D. *et al.* What is—and what is not—an optical isolator. *Nature Photon.* **7,** 579–582 (2013).
10. Fan, S. *et al.* Comment on 'Nonreciprocal light propagation in a silicon photonic circuit'. *Science* **335,** 38 (2012).
11. Iwamura, H., Hayashi, S. & Iwasaki, H. A compact optical isolator using a $Y_3Fe_5O_{12}$ crystal for near infra-red radiation. *Opt. Quantum Electron.* **10,** 393–398 (1978).
12. Shiraishi, K., Sugaya, S. & Kawakami, S. Fiber Faraday rotator. *Appl. Opt.* **23,** 1103–1106 (1984).
13. Gauthier, D., Narum, P. & Boyd, R. Simple, compact, high-performance permanent-magnet Faraday isolator. *Opt. Lett.* **11,** 623–625 (1986).
14. Shoji, Y., Mizumoto, T., Yokoi, H., Hsieh, I. & Osgood, R. Magneto-optical isolator with silicon waveguides fabricated by direct bonding. *Appl. Phys. Lett.* **92,** 071117 (2008).
15. Tien, M., Mizumoto, T., Pintus, P., Kromer, H. & Bowers, J. Silicon ring isolators with bonded nonreciprocal magneto-optic garnets. *Opt. Express* **19,** 11740–11745 (2011).
16. Bi, L. *et al.* On-chip optical isolation in monolithically integrated non-reciprocal optical resonators. *Nature Photon.* **5,** 758–762 (2011).
17. Ghosh, S. *et al.* Ce:YIG/silicon-on-insulator waveguide optical isolator realized by adhesive bonding. *Opt. Express* **20,** 1839–1848 (2012).
18. Yu, Z. & Fan, S. Complete optical isolation created by indirect interband photonic transitions. *Nature Photon.* **3,** 91–94 (2009).
19. Kang, M. S., Butsch, A. & Russel, P. Reconfigurable light-driven opto-acoustic isolators in photonic crystal fibre. *Nature Photon.* **5,** 549–553 (2011).
20. Lira, H., Yu, Z., Fan, S. & Lipson, M. Electrically driven nonreciprocity induced by interband photonic transition on a silicon chip. *Phys. Rev. Lett.* **109,** 33901 (2012).
21. Doerr, C. R., Dupius, N. & Zhang, L. Optical isolator using two tandem phase modulators. *Opt. Lett.* **36,** 4293–4295 (2011).

22. Doerr, C. R., Chen, L. & Vermeulen, D. Silicon photonics broadband modulation-based isolator. *Opt. Express* **22,** 4493–4498 (2014).
23. Yu, Z. & Fan, S. Optical isolation based on nonreciprocal phase shift induced by interband photonic transitions. *Appl. Phys. Lett.* **94,** 171116 (2009).
24. Fang, K., Yu, Z. & Fan, S. Photonic Aharonov–Bohm effect based on dynamic modulation. *Phys. Rev. Lett.* **108,** 153901 (2012).
25. Tzuang, L., Fang, K., Nussenzveig, P., Fan, S. & Lipson, M. Non-reciprocal phase shift induced by an effective magnetic flux for light. *Nature Photon.* **8,** 701–705 (2014).
26. Li, E., Eggleton, B., Fang, K. & Fan, S. Photonic Aharonov–Bohm effect in photon–phonon interactions. *Nature Commun.* **5,** 3225 (2014).
27. Sounas, D. L., Caloz, C. & Alu, A. Giant non-reciprocity at the subwavelength scale using angular momentum-biased metamaterials. *Nature Commun.* **4,** 2407 (2013).
28. Boyd, R. *Nonlinear Optics* 3rd edn (Academic, 2008).
29. Siegman, A. E. *Lasers* Ch. 29 (University Science Books, 1986).
30. Berenger, J. P. A perfectly matched layer for the absorption of electromagnetic waves. *J. Comput. Phys.* **114,** 185–200 (1994).
31. Reinke, C. *et al.* Nonlinear finite-difference time-domain method for the simulation of anistropic, $\chi^{(2)}$, and $\chi^{(3)}$ optical effects. *J. Lightw. Technol.* **24,** 624–634 (2006).
32. Gallo, K., Assanto, G., Parameswaran, K. R. & Fejer, M. M. All-optical diode in a periodically poled lithium niobate waveguide. *Appl. Phys. Lett.* **79,** 314–316 (2001).
33. Huang, X. & Fan, S. Complete all-optical silica fiber isolator via stimulated Brillouin scattering. *J. Lightw. Technol.* **29,** 2267–2275 (2011).
34. Poulton, C. *et al.* Design for broadband on-chip isolator using stimulated Brillouin scattering in dispersion-engineered chalcogenide waveguides. *Opt. Express* **20,** 21236 (2012).

Acknowledgements

This work was supported in part by the US Air Force Office of Scientific Research (grant no. FA9550-09-1-0704) and the US National Science Foundation (grant no. ECCS-1201914). Y.S. also acknowledges the support of a Stanford Graduate Fellowship.

Author contributions

Y.S., Z.Y. and S.F. designed the study and contributed to the analytic derivation. Y.S. wrote the numerical code and performed the simulation. Y.S. and S.F. wrote the manuscript with input from Z.Y., and S.F. supervised the project.

Additional information

Supplementary information is available in the online version of the paper. Reprints and permissions information is available online at www.nature.com/reprints. Correspondence and requests for materials should be addressed to S.F.

Competing financial interests

The authors declare no competing financial interests.

nature photonics

SUPPLEMENTARY INFORMATION

DOI: 10.1038/NPHOTON.2015.79

Limitations of nonlinear optical isolators due to dynamic reciprocity

Yu Shi[1], Zongfu Yu[2] and Shanhui Fan[1]

[1] *Department of Electrical Engineering, Ginzton Laboratory, Stanford University, Stanford, California 94305, USA*

[2] *Department of Electrical and Computer Engineering, University of Wisconsin, Madison, Wisconsin 53706, USA.*

DOI: 10.1038/NPHOTON.2015.79

Part I. Derivation of Eq. (1) from the Maxwell's equations

We begin with the source and current-free Maxwell's equations in a non-magnetic medium:

$$\nabla \cdot \tilde{\mathbf{D}} = 0, \tag{S-1.1}$$

$$\nabla \cdot \tilde{\mathbf{B}} = 0, \tag{S-1.2}$$

$$\nabla \times \tilde{\mathbf{E}} = -\frac{\partial \tilde{\mathbf{B}}}{\partial t}, \tag{S-1.3}$$

$$\nabla \times \tilde{\mathbf{B}} = \mu_0 \frac{\partial \tilde{\mathbf{D}}}{\partial t}. \tag{S-1.4}$$

In a nonlinear medium, the constitutive relationship between $\tilde{\mathbf{D}}$ and $\tilde{\mathbf{E}}$ is described by:

$$\tilde{\mathbf{D}} = \epsilon_0 \tilde{\mathbf{E}} + \tilde{\mathbf{P}} = \epsilon_0 \left(1 + \chi^{(1)}(\mathbf{r})\right) \tilde{\mathbf{E}} + \tilde{\mathbf{P}}^{NL} = \epsilon_0 \epsilon(\mathbf{r}) \tilde{\mathbf{E}} + \tilde{\mathbf{P}}^{NL}, \tag{S-2}$$

where $\epsilon(\mathbf{r}) \equiv 1 + \chi^{(1)}(\mathbf{r})$ captures the linear dielectric response, and $\tilde{\mathbf{P}}^{NL}$ describes the nonlinear polarization density.

We now proceed to derive the wave-nature of the $\tilde{\mathbf{E}}$ by taking the curl of Eq. (S-1.3), and replacing $\nabla \times \tilde{\mathbf{B}}$ by $\mu_0(\partial \tilde{\mathbf{D}}/dt)$ to obtain

$$\nabla \times \nabla \times \tilde{\mathbf{E}} + \mu_0 \frac{\partial^2}{\partial t^2} \tilde{\mathbf{D}} = 0. \tag{S-3}$$

By substituting in the constitutive relationship in Eq. (S-2), we obtain the nonlinear Maxwell's wave equation as described in Eq. (1).

$$\nabla \times \nabla \times \tilde{\mathbf{E}} + \mu_0 \epsilon(\mathbf{r}) \frac{\partial^2 \tilde{\mathbf{E}}}{\partial t^2} = -\mu_0 \frac{\partial^2 \tilde{\mathbf{P}}^{NL}}{\partial t^2}. \tag{S-4}$$

Part II. Non-reciprocity for small additional wave having a spectrum that overlaps with the frequency of the large signal

In this Supplementary Information we consider the issue of reciprocity in the case as depicted in Fig. 2(c), where the small additional wave has a spectrum that overlaps with the frequency of large signal. In general, when linearizing nonlinear Maxwell's equation, the resulting equation may have a form that is different from the Maxwell's equation. Therefore, to discuss the issue of reciprocity for such linearized equations, we need a more general treatment. Consider two vector fields $\mathbf{f}(\mathbf{r})$ and $\mathbf{g}(\mathbf{r})$, we define the inner product of these two vector fields as:

$$\mathbf{f} \cdot \mathbf{g} \equiv \int \mathbf{dr}\ \mathbf{f}(\mathbf{r}) \cdot \mathbf{g}(\mathbf{r}). \tag{S-5}$$

We also define a linear operator $\widehat{\mathbf{O}}$ that map between vector fields:

$$\widehat{\mathbf{O}} \cdot \mathbf{f} \equiv \int \mathbf{dr}'\, \boldsymbol{O}(\mathbf{r}, \mathbf{r}') \cdot\ \mathbf{f}(\mathbf{r}'). \tag{S-6}$$

Consider a system described by

$$\widehat{\mathbf{O}} \cdot \mathbf{E} = \mathbf{J}, \tag{S-7}$$

where $\mathbf{J}$ is a source, and $\mathbf{E}$ is the resulting field. As a definition, such a system is reciprocal if, for two different sources $\mathbf{J}^{(a)}$ and $\mathbf{J}^{(b)}$, the resulting fields $\mathbf{E}^{(a)}$ and $\mathbf{E}^{(b)}$ satisfy the following relation:

$$\mathbf{J}^{(a)} \cdot \mathbf{E}^{(b)} = \mathbf{J}^{(b)} \cdot \mathbf{E}^{(a)}. \tag{S-8}$$

One can prove that the system is reciprocal, if and only if $\widehat{\mathbf{O}}$ is a symmetric operator, i.e.

$$\mathbf{f} \cdot \left(\widehat{\mathbf{O}} \cdot \mathbf{g}\right) = \mathbf{g} \cdot \left(\widehat{\mathbf{O}} \cdot \mathbf{f}\right) \tag{S-9}$$

for arbitrary pair of fields $\mathbf{f}$ and $\mathbf{g}$. The treatment here reduces to the standard treatment of Lorentz reciprocity when $\widehat{\mathbf{O}}$, $\mathbf{f}$, and $\mathbf{g}$ in Eq. (S-9) are the standard operator from the Maxwell's equation, electric current source, and electric field, respectively.

We now develop the linearized equation for the additional small-amplitude wave as depicted in Fig. 2(c). As it turns out, for this case it is sufficient to consider the additional small-amplitude wave with two frequencies ω_1 and ω_2 (red arrows, Fig. 2c), satisfying $\omega_1 + \omega_2 = 2\omega_0$, where ω_0 is the frequency of the large signal.

Analytically, the $\mathbf{E}$ field in this system can be represented as:

DOI: 10.1038/NPHOTON.2015.79

$$\tilde{\mathbf{E}} = \tilde{\mathbf{E}}_0 + \tilde{\mathbf{E}}_1 + \tilde{\mathbf{E}}_2 = \mathbf{E}_0 e^{i\omega_p t} + \mathbf{E}_1 e^{i\omega_1 t} + \mathbf{E}_2 e^{i\omega_2 t} + \mathbf{c.c.}, \tag{S-10}$$

where $\mathbf{E}_0 \gg \mathbf{E}_1, \mathbf{E}_2$. Upon linearizing the nonlinear wave equation by keeping only terms to the first order of $\mathbf{E}_1$ and $\mathbf{E}_2$, we find that the polarization density at the signal frequencies ω_1 and ω_2 are:

$$\begin{aligned}\tilde{\mathbf{P}}^{NL}(\omega_1) &= \epsilon_0\chi^{(3)}\left(6|\mathbf{E}_0|^2\mathbf{E}_1 + 3\mathbf{E}_0{}^2\mathbf{E}_2^*\right)e^{i\omega_1 t} + \epsilon_0\chi^{(3)}\left(6|\mathbf{E}_0|^2\mathbf{E}_1^* + 3\mathbf{E}_0^{*2}\mathbf{E}_2\right)e^{-i\omega_1 t},\\ \tilde{\mathbf{P}}^{NL}(\omega_2) &= \epsilon_0\chi^{(3)}\left(6|\mathbf{E}_0|^2\mathbf{E}_2 + 3\mathbf{E}_0{}^2\mathbf{E}_1^*\right)e^{i\omega_2 t} + \epsilon_0\chi^{(3)}\left(6|\mathbf{E}_0|^2\mathbf{E}_2^* + 3\mathbf{E}_0^{*2}\mathbf{E}_1\right)e^{-i\omega_2 t}.\end{aligned} \tag{S-11}$$

Inserting Eqs. (S-10) and (S-11) into the Maxwell's equations

$$\nabla\times\nabla\times\tilde{\mathbf{E}} + \mu_0\epsilon(\mathbf{r})\frac{\partial^2\tilde{\mathbf{E}}}{\partial t^2} + \mu_0\frac{\partial^2\tilde{\mathbf{P}}^{NL}}{\partial t^2} = -\mu_0\frac{\partial\tilde{\mathbf{J}}}{\partial t}, \tag{S-12}$$

where $\tilde{\mathbf{J}}$ is an external source that has components only at ω_1 and ω_2, we arrive at

$$\begin{aligned}&\left(\nabla\times\nabla\times - \omega_1{}^2\mu_0\epsilon(\mathbf{r}) - 6\omega_1{}^2\mu_0\epsilon_0\chi^{(3)}|\mathbf{E}_0|^2\right)\mathbf{E}_1 e^{i\omega_1 t} - 3\omega_1{}^2\mu_0\epsilon_0\chi^{(3)}\mathbf{E}_0{}^2\mathbf{E}_2^* e^{i\omega_1 t}\\ &+\left(\nabla\times\nabla\times - \omega_2{}^2\mu_0\epsilon(\mathbf{r}) - 6\omega_2{}^2\mu_0\epsilon_0\chi^{(3)}|\mathbf{E}_0|^2\right)\mathbf{E}_2 e^{i\omega_2 t} - 3\omega_2{}^2\mu_0\epsilon_0\chi^{(3)}\mathbf{E}_0{}^2\mathbf{E}_1^* e^{i\omega_2 t}\\ &+\mathbf{c.c.}\\ &= -i\mu_0\omega_1\mathbf{J}_1 e^{i\omega_1 t} - i\mu_0\omega_2\mathbf{J}_2 e^{i\omega_2 t} + \mathbf{c.c.}\end{aligned} \tag{S-13}$$

Therefore, we arrive at the frequency-domain equation that describes such small amplitude additional waves:

$$\begin{pmatrix} \nabla\times\nabla\times - \omega_1{}^2\mu_0\epsilon(\mathbf{r}) - 6\omega_1{}^2\mu_0\epsilon_0\chi^{(3)}|\mathbf{E}_0|^2 & 0 & -3\omega_1{}^2\mu_0\epsilon_0\chi^{(3)}\mathbf{E}_0{}^2 & 0\\ 0 & \nabla\times\nabla\times - \omega_2{}^2\mu_0\epsilon(\mathbf{r}) - 6\omega_2{}^2\mu_0\epsilon_0\chi^{(3)}|\mathbf{E}_0|^2 & 0 & -3\omega_2{}^2\mu_0\epsilon_0\chi^{(3)}\mathbf{E}_0{}^2\\ -3\omega_2{}^2\mu_0\epsilon_0\chi^{(3)}\mathbf{E}_0^{*2} & 0 & \nabla\times\nabla\times - \omega_1{}^2\mu_0\epsilon(\mathbf{r}) - 6\omega_1{}^2\mu_0\epsilon_0\chi^{(3)}|\mathbf{E}_0|^2 & 0\\ 0 & -3\omega_1{}^2\mu_0\epsilon_0\chi^{(3)}\mathbf{E}_0^{*2} & 0 & \nabla\times\nabla\times - \omega_2{}^2\mu_0\epsilon(\mathbf{r}) - 6\omega_2{}^2\mu_0\epsilon_0\chi^{(3)}|\mathbf{E}_0|^2 \end{pmatrix}\begin{pmatrix}\mathbf{E}_1\\ \mathbf{E}_2\\ \mathbf{E}_2^*\\ \mathbf{E}_1^*\end{pmatrix}$$

$$= -i\mu_0\begin{pmatrix}\omega_1\mathbf{J}_1\\ \omega_2\mathbf{J}_2\\ -\omega_2\mathbf{J}_2^*\\ -\omega_1\mathbf{J}_1^*\end{pmatrix},$$

which is of the form of Eq. (S-7). Importantly, we note that $\hat{\mathbf{O}}^{\mathrm{T}} \neq \hat{\mathbf{O}}$ since $\omega_1{}^2\mathbf{E}_0{}^2 \neq \omega_2{}^2\mathbf{E}_0^{*2}$. Therefore, in the presence of large-amplitude input, the system is not reciprocal to the small additional waves of the form described in Fig. 2(c).